Spatial Limits to MIMO Capacity in General Scattering Environments

Tony S. Pollock, Thushara D. Abhayapala and Rodney A. Kennedy
National ICT Australia
Locked Bag 8001
Canberra ACT 2601, Australia
tony.pollock@nicta.com.au

***Abstract*—In this paper we present a new upper bound on the capacity of MIMO systems. By characterizing the fundamental communication modes of a physical aperture, we develop an intrinsic capacity which is independent of antenna array geometries and array signal processing. Using a modal expansion for free-space wave propagation we show that there exists a maximum achievable capacity for communication between spatial regions of space, which depends on the size of the regions and the statistics of the scattering environment.**

I. INTRODUCTION

Multiple-Input Multiple-Output (MIMO) communications systems using multi-antenna arrays simultaneously during transmission and reception have generated significant interest in recent years. Theoretical work of [1] and [2] showed the potential for significant capacity increases in wireless channels via spatial multiplexing with sparse antenna arrays. However, in reality the capacity is significantly reduced when the antennas are constrained to spatial regions so the signals received by different antennas become correlated, corresponding to a reduction of the effective number of sub-channels between transmit and receive antennas [3]. Previous studies have given insights and bounds into the effects of correlated channels, [3–6], however most have been for a limited set of channel realizations and antenna configurations.

In contrast, we present a new fundamental upper bound on the capacity of a wireless channel which is independent of antenna array geometries and array signal processing. In this paper we approach the MIMO capacity problem from a physical wave field perspective. By using the underlying physics of free-space wave propagation we can explore the fundamental limits of capacity due to constraints imposed by the basic laws governing wave field behavior. In particular, using a modal expansion for free-space wave propagation we show that there exists a maximum achievable capacity for communication between spatial regions of space, which depends on the size of the regions and the statistics of the scattering environment. This bound on capacity gives the optimal MIMO capacity and thus provides a benchmark for future array and space-time coding developments.

II. CHANNEL MODEL

Consider the 2D MIMO system shown in Fig. 1, where the transmitter consists of n_{T} transmit antennas located within a circular aperture of radius r_{T}. Similarly, at the receiver, there are n_{R} antennas within a circular aperture of radius r_{R}. Denote the n_{T} transmit antenna positions by $\boldsymbol{x}_t = (\|\boldsymbol{x}_t\|, \theta_t)$, $t = 1, 2, \ldots, n_{\mathrm{T}}$, in polar coordinates, relative to the origin of the transmit aperture, and the n_{R} receive antenna positions by $\boldsymbol{y}_r = (\|\boldsymbol{y}_r\|, \varphi_r)$, $r = 1, 2, \ldots, n_{\mathrm{R}}$, relative to the origin of the receive aperture. Note that all transmit and receive antennas are constrained to within the transmit and receive apertures respectively, that is,

$$\|\boldsymbol{x}_t\| \leq r_{\mathrm{T}}, \quad t = 1, 2, \ldots, n_{\mathrm{T}} \tag{1}$$

$$\|\boldsymbol{y}_r\| \leq r_{\mathrm{R}}, \quad r = 1, 2, \ldots, n_{\mathrm{R}}. \tag{2}$$

It is also assumed that the scatterers are distributed in the farfield from all transmit and receive antennas, therefore, define circular scatterer free regions of radius $r_{\mathrm{TS}} > r_{\mathrm{T}}$, and $r_{\mathrm{RS}} > r_{\mathrm{R}}$, such that any scatterers are in the farfield to any antenna within the transmit and receive apertures, respectively.

Finally, the random scattering environment is defined by the effective random complex scattering gain $g(\phi, \psi)$ for a signal leaving from the transmit aperture at an angle ϕ, and entering the receive aperture at an angle ψ, via any number of paths through the scattering environment.

Using this novel model, the wireless channel has been separated into three distinct spatial regions of signal propagation, namely, the transmitter and receiver scatterer free regions which enclose the transmit and receive apertures, and the rest of space assumed to be a general complex scattering media.

Consider the narrowband transmission of n_{T} baseband signals, $\{x_1, x_2, \ldots, x_{n_{\mathrm{T}}}\}$, over a single signalling interval from the n_{T} transmit antennas located within the transmit aperture. From Fig. 1 the noiseless signal

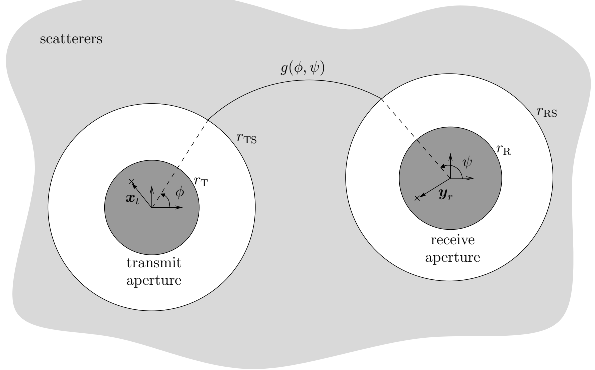

Fig. 1. Scattering model for a 2D flat fading narrowband MIMO system. r_{T} and r_{R} are the radii of circular apertures which contain the transmit and receive antenna arrays, respectively. The radii r_{TS} and r_{RS} describe scatterer free circular regions surrounding the transmit and receive apertures, assumed large enough that any scatterer is farfield to all antennas. The scattering environment is described by $g(\phi,\psi)$ which gives the effective random complex gain for signals departing the transmit aperture from angle ϕ and arriving at the receive aperture from angle ψ, via any number of scattering paths.

at $\boldsymbol{y}_r$ is given by

$$z_r = \sum_{t=1}^{n_{\text{T}}} x_t \iint_{\mathbb{S}^1} g(\phi,\psi)\, e^{ik\|\boldsymbol{x}_t\|\cos(\theta_t-\phi)} \times e^{-ik\|\boldsymbol{y}_r\|\cos(\varphi_r-\psi)}\, d\phi d\psi. \tag{3}$$

where $\mathbb{S}^1$ denotes the unit circle.

Denote $\boldsymbol{x} = [x_1, x_2, \ldots, x_{n_{\text{T}}}]'$ as the column vector of the transmitted signals, and $\boldsymbol{n} = [n_1, n_2, \ldots, n_{n_{\text{R}}}]'$, as the noise vector where n_r is the independent additive white Gaussian noise (AWGN) with variance $N_0 \in \mathcal{N}(0,1)$ at the r-th receive antenna, then the vector of received signals $\boldsymbol{y} = [y_1, y_2, \ldots, y_{n_{\text{R}}}]'$ is given by

$$\boldsymbol{y} = \boldsymbol{H}\boldsymbol{x} + \boldsymbol{n}, \tag{4}$$

where $\boldsymbol{H}$ is the complex random channel matrix with r,t-th element

$$\boldsymbol{H}|_{r,t} = \iint_{\mathbb{S}^1} g(\phi,\psi) e^{ik\|\boldsymbol{x}_t\|\cos(\theta_t-\phi)} \times e^{-ik\|\boldsymbol{y}_r\|\cos(\varphi_r-\psi)}\, d\phi d\psi, \tag{5}$$

representing the channel gain between the t-th transmit antennna and the r-th receive antenna.

Equation (5) allows modelling of the spatial channel for any general array configuration and scattering environment. However, the integral representation is not directly usable in many applications where closed-form channel gain expressions are desired. In the next section, using a modal analysis of plane waves (5) reduces into a form which reveals the underlying spatial structure of the channel gains, giving a decomposition of the channel matrix $\boldsymbol{H}$ which highlights the different effects of signal propagation in each spatial region.

A. Channel Matrix Decomposition

Consider the modal expansion[1] of the plane wave [7]

$$e^{ik\|\boldsymbol{x}\|\cos(\theta_x-\phi)} = \sum_{n=-\infty}^{\infty} i^n J_n(k\|\boldsymbol{x}\|) e^{-in(\theta_x-\phi)}, \tag{6}$$

for vector $\boldsymbol{x} = (\|\boldsymbol{x}\|, \theta_x)$, and $J_n(\cdot)$ are the Bessel functions of the first kind.

Bessel functions $J_n(z)$, $|n|>0$ exhibit spatially high pass behavior, that is, for fixed order n, $J_n(z)$ starts small and becomes significant for arguments $z \approx \mathcal{O}(n)$. Therefore, for a fixed argument z, the Bessel function $J_n(z) \approx 0$ for all but a finite set of low order modes $n \leq N$, hence (6) is well approximated by the finite sum

$$e^{ik\|\boldsymbol{x}\|\cos(\theta_x-\phi)} = \sum_{n=-N}^{N} \overline{\mathcal{J}_n(\boldsymbol{x})} e^{in\phi}, \tag{7}$$

where $\overline{f(\cdot)}$ is the complex conjugate of function $f(\cdot)$, and define

$$\mathcal{J}_n(\boldsymbol{x}) \triangleq J_n(k\|\boldsymbol{x}\|) e^{in(\phi_x-\pi/2)}, \tag{8}$$

as the *spatial-to-mode* function which maps the sampling point $\boldsymbol{x}$ to the nth mode of the expansion (6). In [8] it was shown that $J_n(z) \approx 0$ for $n > \lceil ze/2 \rceil$, with $\lceil\cdot\rceil$ the ceiling operator. Therefore, we can define

$$N_{\text{T}} \triangleq \lceil \pi e r_{\text{T}}/\lambda \rceil, \tag{9}$$

$$N_{\text{R}} \triangleq \lceil \pi e r_{\text{R}}/\lambda \rceil, \tag{10}$$

such that the truncated expansions

$$e^{ik\|\boldsymbol{x}_t\|\cos(\theta_t-\phi)} = \sum_{n=-N_{\text{T}}}^{N_{\text{T}}} \overline{\mathcal{J}_n(\boldsymbol{x}_t)} e^{in\phi}, \tag{11}$$

$$e^{-ik\|\boldsymbol{y}_r\|\cos(\varphi_r-\psi)} = \sum_{m=-N_{\text{R}}}^{N_{\text{R}}} \mathcal{J}_m(\boldsymbol{y}_r) e^{-in\psi}, \tag{12}$$

hold for every antenna within the transmit and receive apertures of radius r_{T} and r_{R}, respectively.

Substitution of (11) and (12) into (5), gives the closed-form expression for the channel gain between the t-th transmit antenna and r-th receive antenna as

$$\boldsymbol{H}|_{r,t} = \sum_{n=-N_{\text{T}}}^{N_{\text{T}}} \sum_{m=-N_{\text{R}}}^{N_{\text{R}}} \overline{\mathcal{J}_n(\boldsymbol{x}_t)} \mathcal{J}_m(\boldsymbol{y}_r) \times \iint_{\mathbb{S}^1} g(\phi,\psi) e^{in\phi} e^{-im\psi} d\phi d\psi. \tag{13}$$

[1] Each mode, indexed by n, corresponds to a different solution of the governing electromagnetic equations (Maxwell's equations) for the given boundary conditions.

From (13) the channel matrix $\boldsymbol{H}$ can be decomposed into a product of three matrices, which correspond to the three spatial regions of signal propagation,

$$\boldsymbol{H} = \boldsymbol{J}_{\mathrm{R}} \boldsymbol{H}_{\mathrm{S}} \boldsymbol{J}_{\mathrm{T}}^{\dagger}, \tag{14}$$

where $\boldsymbol{J}_{\mathrm{T}}$ is the $n_{\mathrm{T}} \times (2N_{\mathrm{T}}+1)$ *transmit aperture sampling* matrix,

$$\boldsymbol{J}_{\mathrm{T}} = \begin{bmatrix} \mathcal{J}_{-N_{\mathrm{T}}}(\boldsymbol{x}_1) & \cdots & \mathcal{J}_{N_{\mathrm{T}}}(\boldsymbol{x}_1) \\ \mathcal{J}_{-N_{\mathrm{T}}}(\boldsymbol{x}_2) & \cdots & \mathcal{J}_{N_{\mathrm{T}}}(\boldsymbol{x}_2) \\ \vdots & \ddots & \vdots \\ \mathcal{J}_{-N_{\mathrm{T}}}(\boldsymbol{x}_{n_{\mathrm{T}}}) & \cdots & \mathcal{J}_{N_{\mathrm{T}}}(\boldsymbol{x}_{n_{\mathrm{T}}}) \end{bmatrix}, \tag{15}$$

which describes the sampling of the transmit aperture, $\boldsymbol{J}_{\mathrm{R}}$ is the $n_{\mathrm{R}} \times (2N_{\mathrm{R}}+1)$ *receive aperture sampling* matrix,

$$\boldsymbol{J}_{\mathrm{R}} = \begin{bmatrix} \mathcal{J}_{-N_{\mathrm{R}}}(\boldsymbol{y}_1) & \cdots & \mathcal{J}_{N_{\mathrm{R}}}(\boldsymbol{y}_1) \\ \mathcal{J}_{-N_{\mathrm{R}}}(\boldsymbol{y}_2) & \cdots & \mathcal{J}_{N_{\mathrm{R}}}(\boldsymbol{y}_2) \\ \vdots & \ddots & \vdots \\ \mathcal{J}_{-N_{\mathrm{R}}}(\boldsymbol{y}_{n_{\mathrm{R}}}) & \cdots & \mathcal{J}_{N_{\mathrm{R}}}(\boldsymbol{y}_{n_{\mathrm{R}}}) \end{bmatrix}, \tag{16}$$

which describes the sampling of the receive aperture, and $\boldsymbol{H}_{\mathrm{S}}$ is a $(2N_{\mathrm{R}}+1) \times (2N_{\mathrm{T}}+1)$ *scattering environment* matrix, with p,q-th element

$$\boldsymbol{H}_{\mathrm{S}}|_{p,q} = \iint_{\mathbb{S}^1} g(\phi,\psi) e^{i(q-N_{\mathrm{T}}-1)\phi} e^{-i(p-N_{\mathrm{R}}-1)\psi} d\phi d\psi, \tag{17}$$

representing the complex gain between the $(q-N_{\mathrm{T}}-1)$-th mode of the transmit aperture and the $(p-N_{\mathrm{R}}-1)$-th mode of the receive aperture[2].

The channel matrix decomposition (14) separates the channel into three distinct regions of signal propagation: free space transmitter region, scattering region, and free space receiver region, as shown in Fig. 1. The transmit aperture and receive aperture sampling matrices, $\boldsymbol{J}_{\mathrm{T}}$ and $\boldsymbol{J}_{\mathrm{R}}$, describe the mapping of the transmitted signals to the modes of the system, and the modes to received signals, given the respective positions of the antennas, and are constant for fixed antenna locations within the spatial apertures. Conversely, for a random scattering environment the scattering channel matrix $\boldsymbol{H}_{\mathrm{S}}$ will have random elements.

III. Mode-to-Mode Communication

It is well known that the rank of the channel matrix $\boldsymbol{H}$ gives the effective number of independent parallel channels between the transmit and receive antenna arrays, and thus determines the capacity of the system. For the decomposition (14) we have $\mathrm{rank}(\boldsymbol{H}) = \min\{\mathrm{rank}(\boldsymbol{J_T}), \mathrm{rank}(\boldsymbol{J_R}), \mathrm{rank}(\boldsymbol{H}_{\mathrm{S}})\}$, which, for a large number of antennas, becomes $\min\{2N_{\mathrm{T}}+1, 2N_{\mathrm{R}}+1, \mathrm{rank}(\boldsymbol{H}_{\mathrm{S}})\}$. Therefore we see that the number of available modes for the transmit and receive apertures, determined by the size of the apertures, and any possible modal correlation or key-hole effects [9] (loss in $\boldsymbol{H}_{\mathrm{S}}$ rank) limit the capacity of the system, regardless of how many antennas are packed into the apertures.

Assume $n_{\mathrm{T}} = 2N_{\mathrm{T}}+1$ and $n_{\mathrm{R}} = 2N_{\mathrm{R}}+1$ antennas are optimally placed (ideal spatial-to-mode coupling - see Section V) within the transmit and receive regions of radius r_{T} and r_{R}, respectively, with total transmit power P_{T}. In this situation $\boldsymbol{J}_{\mathrm{T}}\boldsymbol{J}_{\mathrm{T}}^{\dagger} = \boldsymbol{I}$ and $\boldsymbol{J}_{\mathrm{R}}^{\dagger}\boldsymbol{J}_{\mathrm{R}} = \boldsymbol{I}$, hence the transmit and receive aperture sampling matrices are unitary and $\boldsymbol{H}_{\mathrm{S}}$ is then unitarily equivalent to $\boldsymbol{H}$. The instantaneous channel capacity with no channel state information at the transmitter and full channel knowledge at the receiver [2] is then given by

$$C = \log \left| \boldsymbol{I}_{2N_{\mathrm{R}}+1} + \frac{\eta}{2N_{\mathrm{T}}+1} \boldsymbol{H}_{\mathrm{S}} \boldsymbol{H}_{\mathrm{S}}^{\dagger} \right|, \tag{18}$$

where $\eta = P_{\mathrm{T}}/N_0$ is the average SNR at any point within the receive aperture.

The mode-to-mode capacity (18) represents the intrinsic capacity for communication between two spatial apertures, giving the maximum capacity for all possible array configurations and array signal processing. We can see from (9) and (10) that the intrinsic capacity is limited by the size of the regions containing the antenna arrays (number of available modes), and the statistics of the scattering channel matrix (modal correlation).

Although the modes considered here are generated from spatially constrained antenna arrays, recent advances in multi-mode antennas allow for the excitation of several modes of the same frequency on a single antenna [10]. Regardless of the method of excitation, the number of effective modes will generally be restricted by the geometrical properties of the antenna(s), and the capacity of the system limited by the statistics of the mode-to-mode channel matrix $\boldsymbol{H}_{\mathrm{S}}$. Therefore, the mode-to-mode capacity (18) represents an intrinsic, or fundamental capacity for spatially constrained MIMO systems in realistic scattering environments.

Fig. 2 shows the radiation pattern of the first 6 modes of the circular aperture, given by

$$P_n(\phi) = \Re\{e^{in\phi}\}^2 = \cos^2(n\phi). \tag{19}$$

Each mode has a unique radiation pattern, therefore, mode-to-mode communication is effectively a pattern diversity scheme, where the signals obtained by different modes may be combined to yield a diversity gain. However, the level of diversity achieved depends on the correlation between the modes, which strongly depends on the scattering environment as shown in the following section.

[2]It is important to note the distinction between the *mode-to-mode* gains due to the scattering environment described by $\boldsymbol{H}_{\mathrm{S}}$, and the *antenna-to-antenna* channel gains described by $\boldsymbol{H}$.

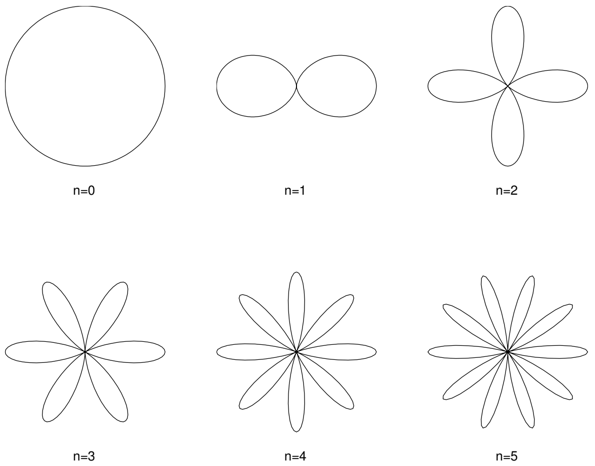

Fig. 2. Radiation patterns of the first 6 modes of a circular aperture.

IV. Properties and Statistics of Scattering Channel Matrix $\boldsymbol{H}_\mathrm{S}$

As the scattering gain function $g(\phi,\psi)$ is periodic with ϕ and ψ it can be expressed using a Fourier expansion. For this 2D model with circular apertures a natural choice of basis functions are the orthogonal circular harmonics $e^{in\phi}$ which form a complete orthogonal function basis set on the unit circle[3], thus express

$$g(\phi,\psi)=\frac{1}{4\pi^2}\sum_{n=-\infty}^{\infty}\sum_{m=-\infty}^{\infty}\beta_m^n e^{-in\phi}e^{im\psi}, \quad (20)$$

with coefficients

$$\beta_m^n=\iint_{\mathbb{S}^1} g(\phi,\psi)e^{in\phi}e^{-im\psi}d\phi d\psi. \quad (21)$$

Therefore, letting $n=q-N_\mathrm{T}-1$, and $m=p-N_\mathrm{R}-1$ denote the transmitter mode and receiver mode index, respectively, the scattering environment matrix coefficients are given by

$$\boldsymbol{H}_\mathrm{S}|_{p,q}=\beta_{p-N_\mathrm{R}-1}^{q-N_\mathrm{T}-1}=\beta_m^n. \quad (22)$$

Thus the random scattering environment can be parameterized by the complex random coefficients β_m^n, $n\in\{-N_\mathrm{T},\ldots,N_\mathrm{T}\}$, $m\in\{-N_\mathrm{R},\ldots,N_\mathrm{R}\}$, which gives the scattering gain between the n-th transmit mode and the m-th receive mode, and $\boldsymbol{H}_\mathrm{S}$ becomes

$$\boldsymbol{H}_\mathrm{S}=\begin{bmatrix}\beta_{-N_\mathrm{R}}^{-N_\mathrm{T}} & \cdots & \beta_{-N_\mathrm{R}}^{N_\mathrm{T}}\\ \beta_{-N_\mathrm{R}+1}^{-N_\mathrm{T}} & \cdots & \beta_{-N_\mathrm{R}+1}^{N_\mathrm{T}}\\ \vdots & \ddots & \vdots\\ \beta_{N_\mathrm{R}}^{-N_\mathrm{T}} & \cdots & \beta_{N_\mathrm{R}}^{N_\mathrm{T}}\end{bmatrix}. \quad (23)$$

Assuming a zero-mean uncorrelated scattering environment (Rayleigh), the scattering channel is characterized by the second-order statistics of the scattering gain function $g(\phi,\psi)$, given by,

$$E\left\{g(\phi,\psi)\overline{g(\phi',\psi')}\right\}=G(\phi,\psi)\delta(\phi-\phi')\delta(\psi-\psi'), \quad (24)$$

where $\delta(\cdot)$ is the Kronecker delta function, and $G(\phi,\psi)=E\left\{|g(\phi,\psi)|^2\right\}$ is the 2D power spectral density (PSD) of the modal correlation function,

$$\begin{aligned}\gamma_{n-n',m-m'} &\triangleq E\left\{\beta_m^n\overline{\beta_{m'}^{n'}}\right\}\\ &=\iint_{\mathbb{S}^1}G(\phi,\psi)e^{i(n-n')\phi}e^{-i(m-m')\psi}d\phi d\psi,\end{aligned} \quad (25)$$

and represents the scattering channel power over departure and arrival angles ϕ and ψ, normalized such that the total scattering channel power

$$\sigma_{\boldsymbol{H}_0}^2=\iint_{\mathbb{S}^1}G(\phi,\psi)d\phi d\psi=1. \quad (26)$$

For the special case of uniform PSD, $G(\phi,\psi)=1/4\pi^2$, the modal correlation becomes

$$\gamma_{n-n',m-m'}=\gamma_{0,0}\delta_{n-n'}\delta_{m-m'}, \quad (27)$$

corresponding to the i.i.d. $\{\beta_n^m\}$ case.

A. Modal Correlation in General Scattering Environments

Define $\mathcal{P}(\psi)$ as the average power density of the scatterers surrounding the receiver, given by the marginalized PSD

$$\mathcal{P}(\psi)\triangleq\int_{\mathbb{S}^1}G(\phi,\psi)\,d\phi, \quad (28)$$

then, from (25) we see the modal correlation between the m and m' communication modes at the receiver is given by

$$\gamma_{m-m'}=\int_{\mathbb{S}^1}\mathcal{P}(\psi)e^{-i(m-m')\psi}d\psi, \quad (29)$$

which gives the modal correlation for all common power distributions $\mathcal{P}(\psi)$: von-Mises, gaussian, truncated gaussian, uniform, piecewise constant, polynomial, Laplacian, Fourier series expansion, etc. Similarly, defining $\mathcal{P}(\phi)$ as the power density of the scatterers surrounding the transmitter, we have the modal correlation at the transmitter

$$\gamma_{n-n'}=\int_{\mathbb{S}^1}\mathcal{P}(\phi)e^{i(n-n')\phi}d\phi. \quad (30)$$

As shown in [4] there is very little variation in the correlation due to the various non-isotropic distributions mentioned above, therefore without loss of generality,

[3] with respect to the natural inner product $\langle f,g\rangle=\int_0^{2\pi}f(\phi)\overline{g(\phi)}d\phi$

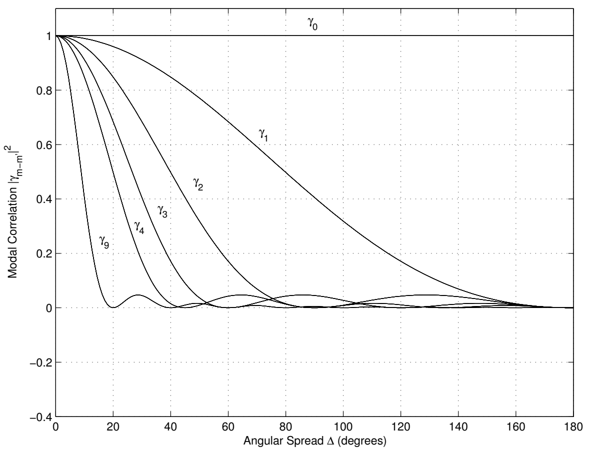

Fig. 3. Modal correlation versus angular spread Δ of a uniform limited power density surrounding the aperture.

we restrict our attention to the case of energy arriving uniformly over limited angular spread Δ around mean ψ_0, i.e., $(\psi_0 - \Delta, \psi_0 + \Delta)$. In this case the modal correlation is given by

$$\gamma_{m-m'} = \mathrm{sinc}((m - m')\Delta)e^{-i(m-m')\psi_0}, \quad (31)$$

which is shown in Fig. 3 for various modes and angular spread. As one would expect, for increasing angular spread we see a decrease in modal correlation, with more rapid reduction for well separated mode orders, e.g. large $|m - m'|$. For the special case of a uniform isotropic scattering environment, $\Delta = \pi$, we have zero correlation between all modes, e.g., $\gamma_{m-m'} = \delta_{m-m'}$.

Fig. 4 shows the impact of modal correlation on the ergodic mode-to-mode capacity for increasing angular spread at the transmitter and isotropic scattering at the reciever[4] for 10dB SNR. We consider transmit and receive apertures of radius 0.8λ, corresponding to $2\lceil \pi e 0.8\rceil + 1 = 15$ modes at each aperture. For comparison, also shown is the capacity for an 15 antenna uniform linear (ULA), uniform circular (UCA), and uniform grid (UGA) arrays, contained within the same aperture size. Also shown is the 15×15 antenna i.i.d. case, corresponding to the rich scattering environment with no restrictions on the antenna placement, i.e., $r_{\mathrm{T}}, r_{\mathrm{R}} \to \infty$.

The mode-to-mode capacity is the maximum achievable capacity between the two apertures, and represents the upper bound on capacity for any antenna array geometry or multi-mode antennas constrained within those apertures. All four cases show no capacity growth for angular spread greater than approximately $60°$, which corresponds to low modal correlations ($\ll 0.5$) for the majority of modes, as seen in Fig. 3.

[4]This models a typical mobile communication scenario, where the receiver is usually surrounded by scatterers, and the base station is mounted high above the scattering environment.

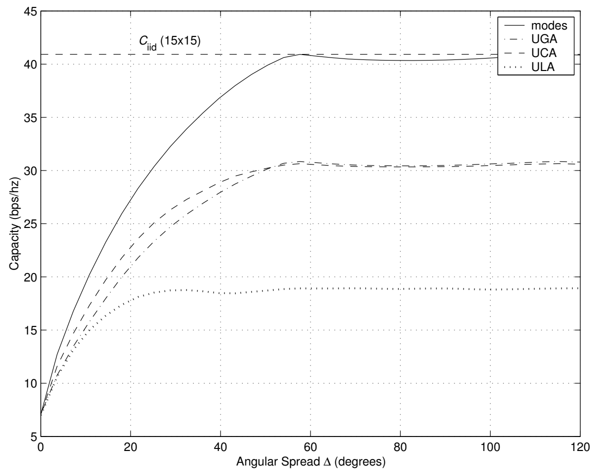

Fig. 4. Capacity versus angular spread at the transmitter for mode-to-mode communication (modes), uniform linear array (ULA), uniform circular array (UCA), and uniform grid array (UGA), within spatial regions of radius 0.8λ and isotropic receiver scattering. The mode-to-mode capacity gives the maximum achievable capacity between the two apertures.

V. Sampling Effects on Capacity

Implementation of a MIMO system requires sampling of the transmit and receive apertures by antenna arrays. Although the mode-to-mode capacity achieves the i.i.d. case, the ULA, UCA and UGA give significantly lower capacity due to poor spatial-to-mode coupling for the given aperture. To observe this, consider the signal leaving the transmit aperture in direction ϕ generated by the n_{T} antennas contained within,

$$\Phi(\phi) = \sum_{t=1}^{n_{\mathrm{T}}} x_t e^{ik\|\boldsymbol{x}_t\|\cos(\theta_t - \phi)} \quad (32)$$

then from (12) and (19) the transmit radiation pattern can be shown to be

$$P(\phi) = E\left\{\Re\{\Phi(\phi)\}^2\right\} \quad (33a)$$

$$= \sum_{n=-N_{\mathrm{T}}}^{N_{\mathrm{T}}} \sigma_n^2 P_n(\phi), \quad (33b)$$

where it is assumed the transmit signals are statistically independent equal power signals. Therefore, one can see that the antenna array excites the $2N_{\mathrm{T}} + 1$ modes of the aperture with $\sigma_n^2 = P_{\mathrm{T}}/n_{\mathrm{T}} \sum_{t=1}^{n_{\mathrm{T}}} |\mathcal{J}_n(\boldsymbol{x}_t)|^2$ power allocated to the n-th mode. Similarly, the antenna array within the receive aperture combines the signals on the $2N_{\mathrm{R}} + 1$ receiver modes with weighting σ_m^2 given to the m-th mode.

In MIMO systems, maximum diversity occurs when there are independent transmit and receive branches, therefore, the maximum capacity will occur for equal power allocation to the full set of uncorrelated modes available for the given aperture size. That is, for an array within a fixed aperture, ideal spatial-to-mode coupling occurs for antenna array geometries such that

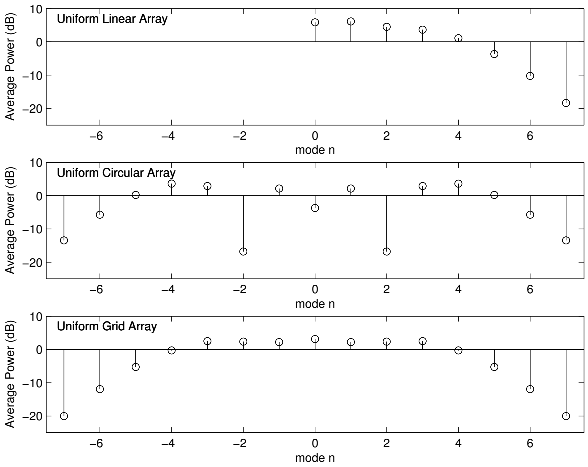

Fig. 5. Average power assigned to each mode for the ULA, UCA, and UGA, within an aperture of 0.8λ, relative to 0dB in each mode for ideal spatial-to-mode coupling.

$\sigma_n^2 = P_{\mathrm{T}}/n_{\mathrm{T}}$ and $\sigma_m^2 = P_{\mathrm{T}}/n_{\mathrm{R}}$ at the transmit and receive apertures respectively. Fig. 5 shows the average power allocation to each mode for the three arrays considered in the previous section, relative to uniform power allocation of 0dB to each mode for ideal spatial-to-mode coupling. Note that due to array symmetry the ULA can only excite $N_{\mathrm{T}}+1$ (resp. $N_{\mathrm{R}}+1$) independent modes of the aperture, therefore the ULA only allocates power to the $n = \{0, \ldots, N_{\mathrm{T}}\}$ modes, giving the poor capacity performance compared to that of the UCA, and UGA. From the UCA and UGA distributions one would expect the UGA to perform better than the UCA, however, although the UCA is less uniform at the lower order modes, it has 5-10dB more power allocated to the higher order modes than that of the UGA. As shown in Section IV-A, well separated modal orders have lower correlation than close modes for smaller angular spreads, hence the UCA distribution predicts better capacity performance for low angular spread, as seen in Fig. 4.

VI. Discussion

We have developed a new upper bound on the capacity for communication between regions in space. Using the underlying physics of free space wave propagation we have shown that there is a fundamental limit to capacity for realistic scattering environments. By characterizing the behavior of possible communication modes for a given aperture, the upper bound on capacity is independent of antenna configurations and array signal processing, and provides a benchmark for future array and space-time coding designs.

In this paper we have restricted the analysis to 2D circular apertures, however, extension to arbitrary shaped regions can be achieved by using a different choice of orthonormal basis functions (e.g. see [11,12]), however, with the exception of spherical apertures [11], finding analytical solutions for more general volumes poses a much harder problem.

References

[1] E. Telatar, "Capacity of multi-antenna gaussian channels," Tech. Rep., ATT Bell Labs, 1995.

[2] G. J. Foschini and M. J. Gans, "On limits of wireless communications in a fading environment when using multiple antennas," *Wireless Personal Communications*, vol. 6, no. 3, 1998.

[3] Da-Shan Shiu, G.J. Foschini, M.J. Gans, and J.M. Kahn, "Fading correlation and its effect on the capacity of multielement antenna systems," *IEEE Transactions on Communications*, vol. 48, no. 3, pp. 502–513, 2000.

[4] T.S. Pollock, T.D. Abhayapala, and R.A. Kennedy, "Introducing space into MIMO capacity calculations," *Journal on Telecommunications Systems*, vol. 24, no. 2-4, pp. 415–436, 2003.

[5] S. Loyka and A. Kouki, "New compound upper bound on mimo channel capacity," *IEEE Communications Letters*, vol. 6, no. 3, pp. 96–98, 2002.

[6] C. Chen-Nee, D.N.C. Tse, J.M. Kahn, and R.A. Valenzuela, "Capacity scaling in mimo wireless systems under correlated fading," *IEEE Transactions on Information Theory*, vol. 48, no. 3, pp. 637–650, 2002.

[7] D. Colton and R. Kress, *Inverse acoustic and elctromagnetic scattering theory*, Springer-Verlag, Berlin, 1992.

[8] H.M. Jones, R.A. Kennedy, and T.D. Abhayapala, "On the dimensonality of multipath fields: spatial extent and richness," in *ICASSP 2002*, Florida, 2002.

[9] D. Chizhik, G.J. Foschini, M.J. Gans, and J.M. Kahn, "Capacities of multi-antenna transmit and receive antennas: correlation and keyholes," *Electronics Letters*, vol. 36, no. 13, pp. 1099–1100, 2000.

[10] F. Demmerle and W. Wiesbeck, "A biconical multibeam antenna for space-division multiple access," *IEEE Transactions on Antennas and Propagation*, vol. 46, no. 6, pp. 782–787, 1998.

[11] T.D. Abhayapala, T.S. Pollock, and R.A. Kennedy, "Novel 3D spatial wireless channel model," in *IEEE Vehicular Technology Conference (Fall)*, Orlando, Florida, USA, 2003.

[12] D. A. B. Miller, "Spatial channels for communicating with waves between volumes," *Optics Letters*, vol. 23, pp. 1645–1647, 1998.